Transaction B: Mechanical Engineering
Vol. 17, No. 6, pp. 456–467
© Sharif University of Technology, December 2010

SCIENTIA IRANICA

Analysis of Manipulators Using SDRE: A Closed Loop Nonlinear Optimal Control Approach

M.H. Korayem[1,*], M. Irani[1] and S. Rafee Nekoo[1]

Abstract. *In this paper, the State Dependent Riccati Equation (SDRE) method is implemented on robotic systems such as a mobile two-links planar robot and a fixed 6R manipulator with complicated dynamic equations. Dynamic modelings of both cases are presented using the Lagrange method. Afterwards, the Dynamic Load Carrying Capacity (DLCC), which is an important characteristic of robots, is calculated for these two systems. DLCC is calculated for the predefined end-effector path, where motor torque limits and tracking error constraints are imposed for this calculation. For a mobile two-links planar robot, the stability constraint is discussed by applying a zero moment point approach. A nonlinear feedback control law is designed for the fully nonlinear dynamics of two cases using a nonlinear closed-loop optimal control method. For solving the SDRE equation that appears in the optimal control solution, a power series approximation method is applied. DLCC is obtained, subject to accuracy and torque constraints, by applying this feedback control law for the square and linear path of the end-effector for mobile two-link and a 6R manipulator, respectively. Finally, simulations are done for both cases and the DLCC of manipulators is determined. Also, actual end-effector positions, required control efforts and the angular position and velocity of joints are presented for full load conditions, and results are discussed*

Keywords: *Mobile manipulator; 6R robot; Nonlinear optimal control; DLCC; SDRE.*

INTRODUCTION

In the last few years, developments in the industrial production of complicated parts and the importance of rapid productions, lead to automatic manufacturing. Manipulators and robot arms helped to achieve this purpose. Furthermore, some activities, like the transportation of heavy pieces and work in dangerous environments and large spaces, led to the use of mobile robots and manipulators.

Whereas mobile manipulators have a higher degree of freedom path planning, the trajectory control and determining of the important parameters of a robot are complicated. One of these important parameters is the Dynamic Load Carrying Capacity (DLCC), the load that a robot can repeatedly lift and carry on a desired trajectory. Korayem and Pilechian [1] calculated the DLCC of flexible joint robots using a sliding mode control for the trajectory tracking problem. Korayem et al. [2] presented the DLCC of flexible joint robots with a feedback linearization method and compared it with an open loop method. Also, Korayem and Irani [3] found the DLCC of mobile manipulators using a nonlinear optimal feedback controller. The solution method is a successful approximation for solving optimal control problems.

In [4], the Iterative Linear Programming (ILP) method is used to solve the optimization problem of finding the DLCC of cable driven robots. The results of the ILP method are then compared with the optimal control method.

In [5], the DLCC of a flexible link manipulator mounted on a vehicle is determined via a feedback linearization control approach. Korayem et al. [6] calculated the maximum allowable load for a flexible link manipulator with a mobile base, applying the finite element approach. This approach is applied to linear and circular trajectories.

Korayem et al. [7] established the maximum load carrying capacity of a mobile robot in an environment with obstacles using an open loop optimal control approach and considered stability constraint. The

1. *Robotic Research Laboratory, College of Mechanical Engineering, Iran University of Science and Technology, Tehran, P.O. Box 18846, Iran.*
*. *Corresponding author. E-mail: hkorayem@iust.ac.ir*

Received 31 January 2010; received in revised form 11 June 2010; accepted 6 September 2010

stability constraint was measured by computing the zero moment point.

In this paper, the optimal control method is used to design a nonlinear closed loop control law for both fixed and mobile manipulators. A proper approach in the nonlinear optimal control method is the SDRE method, based on solving the nonlinear state-dependent Riccati equation. Being simple and systematic are two advantages of this solution method. Also, this method is applicable to fully nonlinear dynamic models. Pearson [8] proposed the SDRE method, which was, then, developed by Wernli and Cook [9]. Then, SDRE was used as nonlinear optimal regulator. Cloutier [10] presented this method with state constraint and compared it with an LQR approach. In [11], the SDRE method is used to synthesize a path controller, and then the simulation results were checked by experimental results using real hardware. Innocenti et al. [12] presented the SDRE method to control a two-link under-actuated robot and described that, with the same designing parameters, the SDRE control can perform better than the LQR control.

Xin et al. [13] used the SDRE method to control a robot. An extra controller based on a neural network is used in the presence of parameter uncertainties to provide robustness characteristics. Shawky et al. [14] represented this method for a flexible link manipulator. For this purpose, the Lagrange and assume mode methods are used for finding the dynamic model. Singh et al. [15] expressed the control of an inverted pendulum on a cart using the SDRE method; different values for weighing matrixes are used and results are compared. In [16] Cimen presented an overview on SDRE with details on stability, optimality and etc. Beikzadeh and Taghirad [17] used this for controlling a permanent magnet synchronous motor.

The exact solution of an SDRE equation is possible for a simple system, but for complicated systems, solving SDRE is difficult and is usually done using numerical methods. In this paper, a power series approximation is applied to solve this problem. The second section presents the method of solving a nonlinear optimal control problem using the SDRE approach. Then, in the next section, the power series approximation method is applied for solving the complex Riccati equation that appeared in the SDRE method. The definitions of a dynamic load carrying capacity and zero moment point are exposed in the next section. Afterwards, the dynamic modeling of a planar, 2-link mobile manipulator and a six degree of freedom manipulator are considered. The last section deals with the implementation of the SDRE method for a mobile manipulator and a 6R robot, and then results for a predefined trajectory are demonstrated.

STATE-DEPENDENT RICCATI EQUATION

Consider a nonlinear equation of a system as below:

$$\dot{x} = f(x(t)) + B(x(t))u(t), x(0) = x_0, \tag{1}$$

where x and u are state and input vectors, respectively, $x \in R^n$ and $u \in R^m$, $f : R^n \rightarrow R^n$, and $B : R^n \rightarrow R^{n\times m}$ are nonlinear functions and x_0 is initial condition. The performance index that must be minimized is of the form:

$$J = \int_0^\infty (x^T(t)Q(x)x(t) + u^T(t)R(x)u(t))dt, \tag{2}$$

where $Q \in R^{n\times n}$ is Symmetric Positive Semi-Definite (SPSD), and $R \in R^{m\times m}$ is Symmetric Positive Definite (SPD). Rewriting the nonlinear equation in the State-Dependent Coefficient (SDC) form becomes [18]:

$$\dot{x} = A(x)x(t) + B(x)u(t). \tag{3}$$

Then the optimal solution of Equation 3, which minimizes the performance index, is obtained from the following equation [18]:

$$X(x)A(x) + A^T(x)X(x) - X(x)B(x)R^{-1}(x)B^T(x)X(x) + Q = 0. \tag{4}$$

This equation is named the state-dependent Riccati equation, where X is symmetric positive definite, which is the solution of the SDRE equation. Also, the state feedback control law is obtained in the following form:

$$u(x) = -R^{-1}(x)B^T(x)X(x)x. \tag{5}$$

POWER SERIES APPROXIMATION METHOD FOR SOLVING SDRE

For finding the numerical solution of SDRE, consider a system with Equation 3 where B is a constant matrix. By rewriting A in the following form [19];

$$A(x) = A_0 + \varepsilon\Delta A(x), \tag{6}$$

and representing X as a Taylor series:

$$X(x,\varepsilon) = \sum_{n=0}^{\infty} \varepsilon^n L_n(x) = X(x)\Big|_{\varepsilon=0} \varepsilon + \frac{\partial^2 X(x)}{\partial \varepsilon^2}\Big|_{\varepsilon=0} \frac{\varepsilon^2}{2} + \ldots \tag{7}$$

and substituting $A(x)$, $X(x,\varepsilon)$ into the SDRE equation, the result will be in the following form:

$$\left(\sum_{n=0}^{\infty}\varepsilon^n L_n(x)\right).(A_0+\varepsilon\Delta A(x)) + (A_0+\varepsilon\Delta A(x))^T\left(\sum_{n=0}^{\infty}\varepsilon^n L_n(x)\right) - \left(\sum_{n=0}^{\infty}\varepsilon^n L_n(x)\right)BR^{-1}B^T\left(\sum_{n=0}^{\infty}\varepsilon^n L_n(x)\right) + Q = 0. \quad (8)$$

By expanding this equation and collecting a similar power of ε, three iterative equations are generated:

$$L_0A_0 + A_0^TL_0 - L_0BR^{-1}B^TL_0 + Q = 0, \quad (9)$$

$$L_0\Delta A(x) + \Delta A(x)^TL_0 + L_1(A_0 - BR^{-1}B^TL_0) + (A_0^T - L_0BR^{-1}B^T)L_1 = 0, \quad (10)$$

$$L_{n-1}\Delta A(x) + \Delta A(x)^TL_{n-1} + L_n(A_0 - BR^{-1}B^TL_0) + (A_0^T - L_0BR^{-1}B^T)L_n - \sum_{m=1}^{n-1}L_mBR^{-1}B^TL_{n-m} = 0, \quad (11)$$

where $n = 2, 3, 4, \cdots$.

The first equation is an Algebraic Riccati Equation (ARE), the second and third are state-dependent Lyapunov equations. These equations are simplified by substitution:

$\Delta A(x) = g(x)\Delta A$:

$$L_0A_0 + A_0^TL_0 - L_0BR^{-1}B^TL_0 + Q = 0, \quad (12)$$

$$L_0\Delta A + \Delta A^TL_0 + L_1(A_0 - BR^{-1}B^TL_0) + (A_0^T - L_0BR^{-1}B^T)L_1 = 0, \quad (13)$$

$$L_{n-1}\Delta A + \Delta A^TL_{n-1} + L_n(A_0 - BR^{-1}B^TL_0) + (A_0^T - L_0BR^{-1}B^T)L_n - \sum_{m=1}^{n-1}L_mBR^{-1}B^TL_{n-m} = 0. \quad (14)$$

Similarly, the state-feedback control law is obtained:

$$u = -R^{-1}B^T\sum_{n=0}^{\infty}g^n(x)L_nx. \quad (15)$$

For most complicated systems, $A(x)$ could not be rewritten as $\Delta A(x) = g(x)\Delta A$. For these systems, $A(x)$ is changed to:

$$A(x) = A_0 + \sum_{i=1}^{j}f_i(x)\Delta A_i, \quad (16)$$

where j is the number of nonlinear terms, and $f_i(x)$ and ΔA_i are constant matrixes. Also, L_1 can be written as:

$$L_1 = \sum_{i=1}^{j}f_i(x)L_1^j. \quad (17)$$

Using two prior terms of the SDRE equation, $L_0, L_1^1, \cdots, L_1^j$ are computed from the equations below:

$$L_0A_0 + A_0^TL_0 - L_0BR^{-1}B^TL_0 + Q = 0, \quad (18)$$

$$L_0\Delta A^j + (\Delta A^T)^jL_0 + L_1^j(A_0 - BR^{-1}B^TL_0) + (A_0^T - L_0BR^{-1}B^T)L_1^j = 0. \quad (19)$$

Finally, the control law can be obtained as:

$$u = -R^{-1}B^T\left(L_0 + \sum_{i=1}^{j}f_i(x)L_1^j\right)x. \quad (20)$$

DYNAMIC LOAD CARRYING CAPACITY

The dynamic load carrying capacity is described as being the maximum load that a manipulator can repeatedly lift and carry on the extended configuration. The DLCC of a fixed 6R manipulator and a two-link planar mobile robot is calculated, with respect to the limitation of motors, tracking error and additional stability constraint. Upper and lower limits of motor torques can be computed from:

$$U_{\max} = U_s - \frac{U_s}{\omega_s}\omega, \quad (21)$$

$$U_{\min} = -U_s - \frac{U_s}{\omega_s}\omega. \quad (22)$$

In the above equation, U_s is the stall torque of a motor and ω_s is no load speed.

The tracking error is calculated as:

$$E = \sqrt{(x_e - x_d)^2 + (y_e - y_d)^2 + (z_e - z_d)^2}, \quad (23)$$

where x, y and z are components of the actual position of the end-effector and x_d, y_d and z_d are components

of the desired position. This error must be bounded during motion as:

$$E \leq \delta. \tag{24}$$

δ is the allowable error for tracking.

The stability constraint is defined by computing the zero moment point. ZMP is the point on the ground where the summation of external forces, moments of inertia and gravity forces are equal to zero. Formulas for ZMP are [7]:

$$x_{zmp} = \frac{\sum_i m_i(\ddot{z}_i + g)x_i - \sum_i m_i \ddot{x}_i z_i - \sum_i (T_y)_i}{\sum_i m_i(\ddot{z}_i + g)}, \tag{25}$$

$$y_{zmp} = \frac{\sum_i m_i(\ddot{z}_i + g)y_i - \sum_i m_i \ddot{y}_i z_i - \sum_i (T_x)_i}{\sum_i m_i(\ddot{z}_i + g)}, \tag{26}$$

where:

$$T_i = I_i.\dot{\omega}_i + \omega_i \times I_i.\omega_i. \tag{27}$$

Details of each term of Equations 25, 26 and 27 are presented in [20].

DYNAMIC MODELING OF MANIPULATORS

Mobile Robot

Two-link mobile robot that is used in simulations is shown in Figure 1 and the parameters of this robot are presented in Table 1.

The generalized coordinates are chosen as:

$$q = \begin{bmatrix} q_b & q_m \end{bmatrix} = \begin{bmatrix} x_f & y_f & \theta_0 & \theta_1 & \theta_2 \end{bmatrix}. \tag{28}$$

By applying the Lagrange method and computing the position and velocity for each center of mass, the

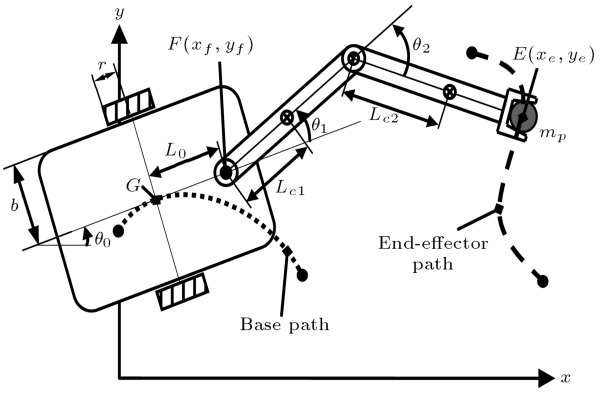

Figure 1. Two-link mobile robot.

Table 1. Parameters of mobile robot.

Parameters	Value	Unit
Length of links	$L_1 = L_2 = 0.5$	M
Center of mass	$L_{c1} = L_{c2} = 0.25$	M
Mass of links	$m_1 = 5,\ m_2 = 3$	kg
Moment of inertia	$I_1 = 0.416,$ $I_2 = 0.0625$	kg.m^2
Mass of wheel	5	kg
Mass of base	94	kg
Moment of inertia of base	$\begin{bmatrix} 0 & 0 & 0 \\ 0 & 0 & 0 \\ 0 & 0 & 6.609 \end{bmatrix}$	kg.m^2
Moment of inertia of wheels	$\begin{bmatrix} 0.131 & 0 & 0 \\ 0 & 0.01 & 0 \\ 0 & 0 & 0.131 \end{bmatrix}$	kg.m^2
b	0.171	M
r	0.075	M
L_0	0.4	M

equations of dynamic motion can be written as:

$$\begin{bmatrix} F_x \\ F_y \\ T_0 \\ \tau_1 \\ \tau_2 \end{bmatrix} = \begin{bmatrix} J_{11} & J_{12} & J_{13} & J_{14} & J_{15} \\ J_{12} & J_{22} & J_{23} & J_{24} & J_{25} \\ J_{13} & J_{23} & J_{33} & J_{34} & J_{35} \\ J_{14} & J_{24} & J_{34} & J_{44} & J_{45} \\ J_{15} & J_{25} & J_{35} & J_{45} & J_{55} \end{bmatrix} \begin{bmatrix} \ddot{x}_f \\ \ddot{y}_f \\ \ddot{\theta}_0 \\ \ddot{\theta}_1 \\ \ddot{\theta}_2 \end{bmatrix} + \begin{bmatrix} C_1 \\ C_2 \\ C_3 \\ C_4 \\ C_5 \end{bmatrix}. \tag{29}$$

Also end-effector coordinates are:

$$\begin{bmatrix} x_e \\ y_e \end{bmatrix} = \begin{bmatrix} x_f + L_1\cos(\theta_0+\theta_1) + L_2\cos(\theta_0+\theta_1+\theta_2) \\ y_f + L_1\sin(\theta_0+\theta_1) + L_2\sin(\theta_0+\theta_1+\theta_2) \end{bmatrix}. \tag{30}$$

In this case, the degree of freedom is $n = 5$ and the end-effector trajectory has $m = 2$ degrees of freedom. Thus, the redundancy of the system is $r = n - m = 3$. The system has one nonholonomic constraint, according to the motion of the mobile base:

$$\dot{x}_f \sin\theta_0 - \dot{y}_f \cos\theta_0 + L_0\dot{\theta}_0 = 0. \tag{31}$$

Two other constraints must be applied for redundancy resolution. A pre-defined path is considered for the base, then $\dot{x}_f$, $\dot{y}_f$, $\ddot{x}_f$ and $\ddot{y}_f$ can be calculated, and θ_0, $\dot{\theta}_0$ and $\ddot{\theta}_0$ are obtained using nonholonomic constraints.

Using the remaining terms of Equation 29, equations of the system are rewritten as:

$$\begin{bmatrix} \tau_1 \\ Sa\tau_2 \end{bmatrix} = \begin{bmatrix} J_{44} & J_{45} \\ J_{45} & J_{55} \end{bmatrix} \begin{bmatrix} \ddot{\theta}_1 \\ \ddot{\theta}_2 \end{bmatrix} + \begin{bmatrix} R_1 \\ R_2 \end{bmatrix}, \tag{32}$$

where:

$$R_1 = J_{14}\ddot{x}_f + J_{24}\ddot{y}_f + J_{34}\ddot{\theta}_0 + C_4, \tag{33}$$

$$R_2 = J_{15}\ddot{x}_f + J_{25}\ddot{y}_f + J_{35}\ddot{\theta}_0 + C_5. \tag{34}$$

6R Fixed Robot

For the second case study, a 6R manipulator as shown in Figure 2, is considered. Also, a schematic view of this manipulator is shown in Figure 3 and Denavit-Hartenberg parameters are demonstrated in Table 2.

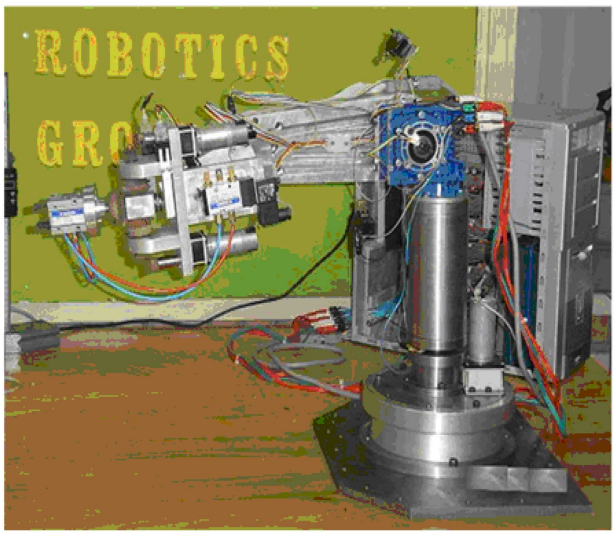

Figure 2. 6R configuration [19].

Table 2. Denavit-Hartenberg parameters of 6R.

Joint	a_i (mm)	d_i (mm)	α_i°	θ_i	Related Link
1	36.5	438	-90	θ_1	Link 1
2	251.5	0	0	θ_2	Link 2
3	125	0	0	θ_3	Link 3
4	92	0	90	θ_4	Gripper YAW
5	0	0	-90	θ_5	Gripper PITCH
6	0	152.8	0	θ_6	Gripper ROLL

The transformation matrix, T, is used for forward kinematic computations [21]:

$$T = \begin{bmatrix} n_x & o_x & a_x & p_x \\ n_y & o_y & a_y & p_y \\ n_z & o_z & a_z & p_z \\ 0 & 0 & 0 & 1 \end{bmatrix}. \tag{35}$$

The elements of T are:

$$\begin{aligned}
n_x &= -c_6 s_1 s_5 + c_1(c_{234}c_5c_6 - s_{234}s_6),\\
n_y &= c_{234}c_5c_6s_1 + c_1c_6s_5 - s_1s_{234}s_6,\\
n_z &= -c_5c_6s_{234} - c_{234}s_6,\\
o_x &= s_1s_5s_6 - c_1(c_6s_{234} + c_{234}c_5s_6),\\
o_y &= -c_6s_1s_{234} - (c_{234}c_5s_1 + c_1s_5)s_6,\\
o_z &= -c_{234}c_6 + c_5s_{234}s_6,\\
a_x &= -c_5s_1 - c_1c_{234}s_5,\\
a_y &= c_1c_5 - c_{234}s_1s_5,\\
a_z &= s_{234}s_5,\\
p_x &= -d_6c_5s_1 + c_1(a_1 + a_2c_2 + a_3c_{23}\\
&\quad + c_{234}(a_4 - d_6s_5)),\\
p_y &= d_6c_1c_5 + s_1(a_1 + a_2c_2 + a_3c_{23}\\
&\quad + c_{234}(a_4 - d_6s_5)),\\
p_z &= d_1 - a_2s_2 - a_3s_{23} + s_{234}(-a_4 + d_6s_5).
\end{aligned} \tag{36}$$

In these equations, a_i and d_i are shown in Figure 3. Also s_i, c_i, s_{ij} and c_{ij} denote $\sin(\theta_i)$, $\cos(\theta_i)$, $\sin(\theta_i+\theta_j)$ and $\cos(\theta_i+\theta_j)$, respectively. The relation between the velocity of an end-effector and the angular velocity of joints is expressed by:

$$V = J\dot{q}. \tag{37}$$

J is the Jacobian matrix of a 6R arm and can be obtained as:

$$J = \begin{bmatrix} j_{11} & j_{12} & j_{13} & j_{14} & j_{15} & 0 \\ j_{21} & j_{22} & j_{23} & j_{24} & j_{25} & 0 \\ 0 & j_{32} & j_{33} & j_{34} & d_6c_5s_{234} & 0 \\ 0 & -s_1 & -s_1 & -s_1 & c_1s_{234} & j_{46} \\ 0 & c_1 & c_1 & c_1 & s_1s_{234} & j_{56} \\ 1 & 0 & 0 & 0 & c_{234} & s_{234}s_5 \end{bmatrix}, \tag{38}$$

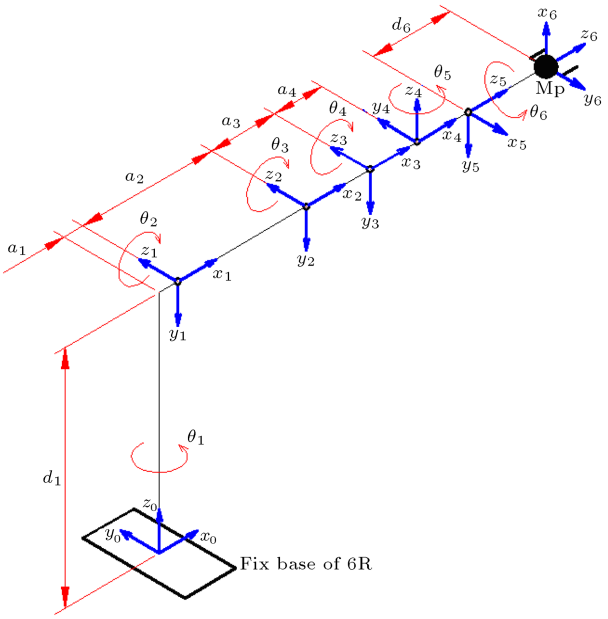

Figure 3. 6R schematic configuration.

where:

$$
\begin{aligned}
j_{11} &= -d_6c_1c_5 - s_1(a_1 + a_2c_2 + a_3c_{23} + c_{234}(a_4 - d_6s_5)),\\
j_{12} &= -c_1(a_2s_2 + a_3s_{23} + s_{234}(a_4 - d_6s_2)),\\
j_{13} &= -c_1(a_3s_{23} + s_{234}(a_4 - d_6s_5)),\\
j_{14} &= c_1s_{234}(-a_4 + d_6s_5),\\
j_{15} &= -d_6c_1c_{234}c_5 + d_6s_1s_5,\\
j_{21} &= -d_6s_1c_5 + c_1(a_1 + a_2c_2 + a_3c_{23} + c_{234}(a_4 - d_6s_5)),\\
j_{22} &= -s_1(a_2s_2 + a_3s_{23} + s_{234}(a_4 - d_6s_5)),\\
j_{23} &= -s_1(a_3s_{23} + s_{234}(a_4 - d_6s_5)),\\
j_{24} &= s_1s_{234}(-a_4 + d_6s_5),\\
j_{25} &= -d_6(c_{234}c_5s_1 + c_1s_5),\\
j_{32} &= -a_2c_2 - a_3c_{23} + c_{234}(-a_4 + d_6s_5),\\
j_{33} &= -a_3c_{23} + c_{234}(-a_4 + d_6s_5),\\
j_{34} &= c_{234}(-a_4 + d_6s_5),\\
j_{46} &= -c_5s_1 - c_1c_{234}s_5,\\
j_{56} &= c_1c_5 - c_{234}s_1s_5.
\end{aligned}
\tag{39}
$$

According to Equations 21 and 22, characteristics of motors U_s and ω_s are needed for dynamic load carrying capacity calculations. These values are determined and collected in Table 3.

Table 3. Motor characteristics for 6R arm.

Joint	U_s (N.m)	ω_s (rad/s)
1	114	1.32
2	98	4.19
3	382.2	0.73
4	19	450.29
5	40.4	9.01
6	40.4	9.01

CONTROL IMPLEMENTATION AND RESULTS

Mobile Robot

For state space representation of a mobile 2-link manipulator, the angular position and velocity of links are chosen as states, as below:

$$
\begin{bmatrix} \theta_1 \\ \dot{\theta}_1 \\ \theta_2 \\ \dot{\theta}_2 \end{bmatrix} = \begin{bmatrix} x_1 \\ x_2 \\ x_3 \\ x_4 \end{bmatrix}. \tag{40}
$$

Thus, the state-space representation is obtained as:

$$
\frac{d}{dt}\begin{bmatrix} x_1 \\ x_2 \\ x_3 \\ x_4 \end{bmatrix} = \begin{bmatrix} x_2 \\ P(J_{55}(U_1 - R_1) - J_{45}(U_2 - R_2)) \\ x_4 \\ P(-J_{45}(U_1 - R_1) + J_{44}(U_2 - R_2)) \end{bmatrix}. \tag{41}
$$

Parameter P in Equation 41 is:

$$
P = \frac{1}{J_{44}J_{55} - J_{45}^2}. \tag{42}
$$

The predefined path for the end-effector is a 1×1 m^2 square and the simulation time is 12 sec. At the beginning of the motion, the end-effector is at the left-hand upper corner of this square and point F at the origin. Also, the base moves from the origin to point (2, 0) and then returns to the origin. The actual end-effector paths under full load conditions and upper and lower limits are shown in Figure 4.

The allowable tracking error in Equation 24 is chosen as $\delta = 0.02$ m and the tracking error is computed according to Equation 23 and plotted in Figure 5. This figure indicates that the maximum error occurred near $t = 4$ sec at the up side of the square. The angular position and velocity of joints are shown in Figures 6 and 7.

In this case, the ZMP plot shows that stability is guaranteed. For stability consideration, changes in zero moment point location during the motion and limits of stability are shown in Figure 8, where the stability margins are virtual lines between wheels and castor.

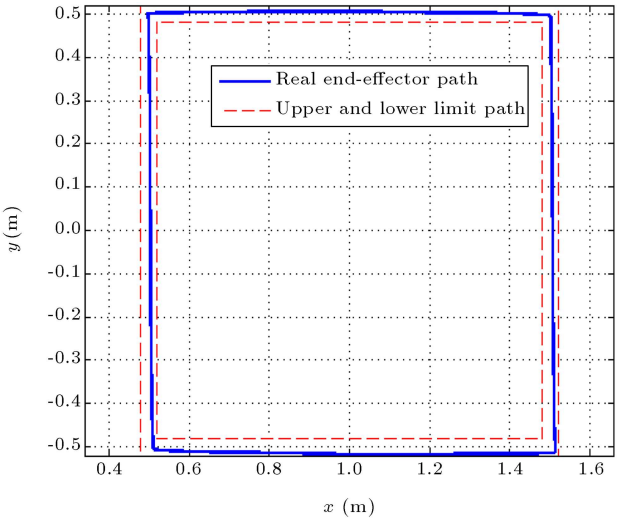

Figure 4. End-effector path.

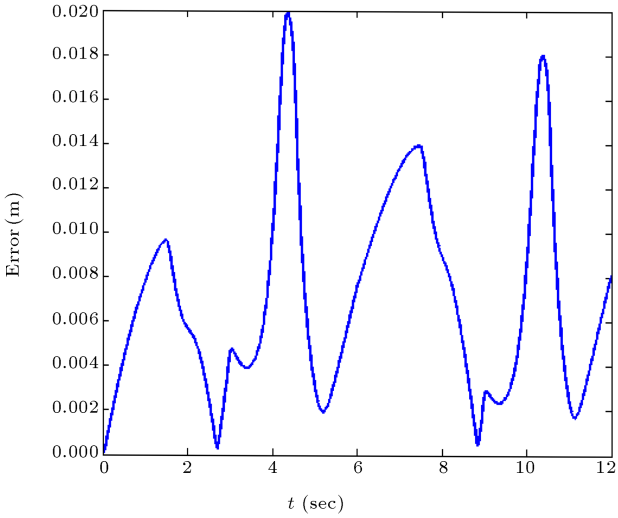

Figure 5. Tracking error.

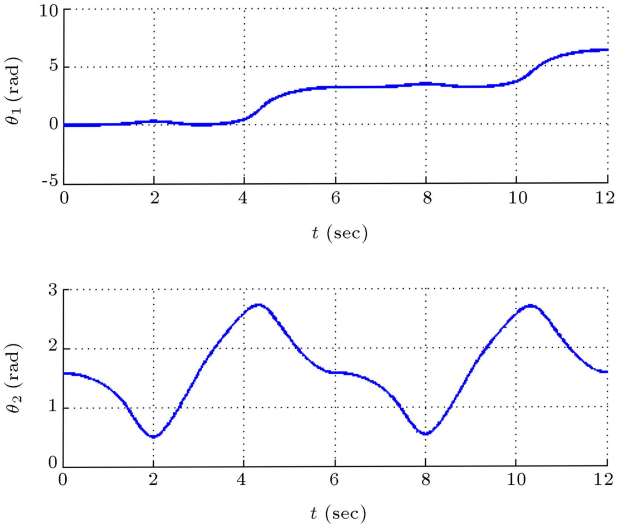

Figure 6. Angular positions.

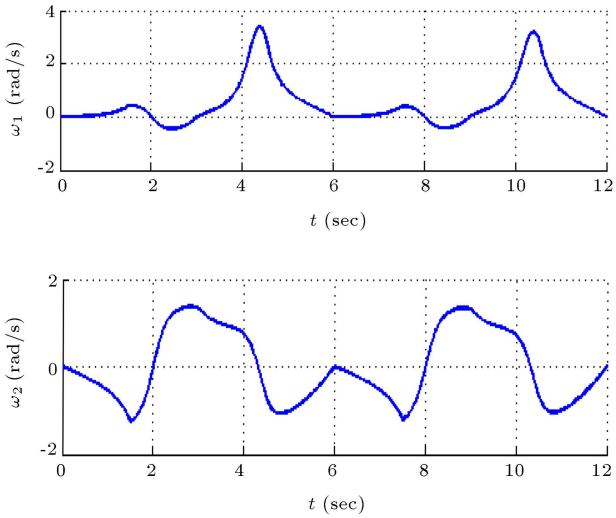

Figure 7. Angular velocity of joints.

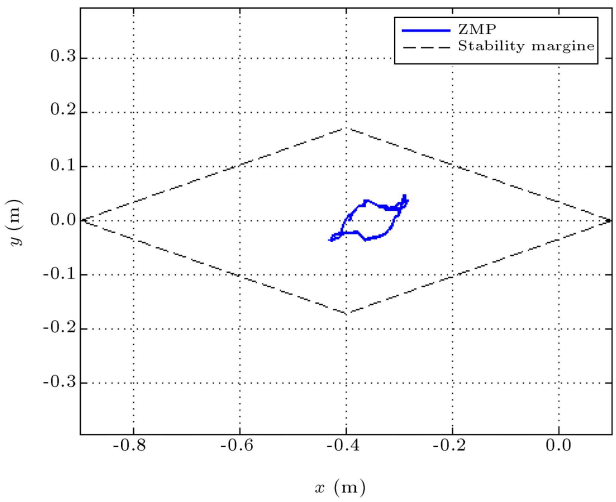

Figure 8. ZMP and stability margin.

Figure 9 demonstrates the torque of motors and the upper and lower bounds of torques, according to Equations 21 and 22. Using torques and tracking constraints, the dynamic load carrying capacity of manipulator is obtained as 6.1 kg.

6R MANIPULATOR

For the second case study, the vector of state variables for a 6R arm is determined as:

$$[X]_{1\times 12} = \begin{bmatrix} q \\ \dot{q} \end{bmatrix}. \tag{43}$$

q is the vector of the angular position of joints:

$$q = \begin{bmatrix} \theta_1 & \theta_2 & \theta_3 & \theta_4 & \theta_5 & \theta_6 \end{bmatrix}. \tag{44}$$

Also $\dot{q}$ is the angular velocities vector:

$$\dot{q} = \begin{bmatrix} \dot{\theta}_1 & \dot{\theta}_2 & \dot{\theta}_3 & \dot{\theta}_4 & \dot{\theta}_5 & \dot{\theta}_6 \end{bmatrix} \tag{45}$$

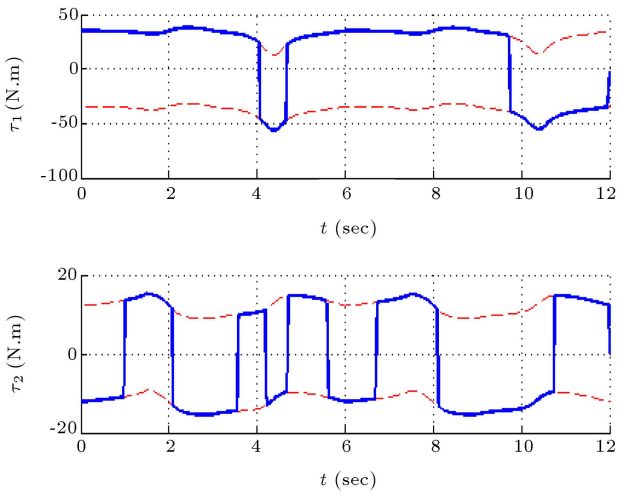

Figure 9. Torques of motors.

Thus, state-space representation is obtained as:

$$\dot{X} = [x_7; x_8; x_9; x_{10}; x_{11}; x_{12}; D^{-1}(U - C - G)]. \quad (46)$$

In Equation 46, D is the inertial matrix, C is the vector of Coriolis and centrifugal forces, G is the gravity force vector and U is the input control vector. Details of these matrix and vectors are as below:

$$D = \begin{bmatrix} d_{11} & d_{12} & d_{13} & d_{14} & d_{15} & d_{16} \\ d_{12} & d_{22} & d_{23} & d_{24} & d_{25} & d_{26} \\ d_{13} & d_{23} & d_{33} & d_{34} & d_{35} & d_{36} \\ d_{14} & d_{24} & d_{34} & d_{44} & d_{45} & d_{46} \\ d_{15} & d_{25} & d_{35} & d_{45} & d_{55} & d_{56} \\ d_{16} & d_{26} & d_{36} & d_{46} & d_{56} & d_{66} \end{bmatrix}, \quad (47)$$

$$C = \begin{bmatrix} \bar{c}_1 & \bar{c}_2 & \bar{c}_3 & \bar{c}_4 & \bar{c}_5 & \bar{c}_6 \end{bmatrix}^T, \quad (48)$$

$$G = \begin{bmatrix} g_1 & g_2 & g_3 & g_4 & g_5 & g_6 \end{bmatrix}^T, \quad (49)$$

$$U = \begin{bmatrix} u_1 & u_2 & u_3 & u_4 & u_5 & u_6 \end{bmatrix}^T. \quad (50)$$

The control vector is computed through the SDRE method using Equation 20. A linear trajectory is selected for the tracking problem that connects initial point $P_0(0.55, -0.1, 0.5)$ and final point $P_f(0.1, -0.3, 0.22)$ at 10 sec. The line is designed so that the velocity and acceleration of the end-effector are zero at both initial and final points. Actual angular velocities of joints are shown in Figures 10 to 12 for full load conditions. These figures imply that the actual angular velocities of joints are zero at initial and final points.

Figures 13 to 15 present the actual angular positions of joints under full load conditions, which indicate a smooth angular motion for joints during the motion. The desired values of angles and angular velocities are computed by solving differential Equation 37.

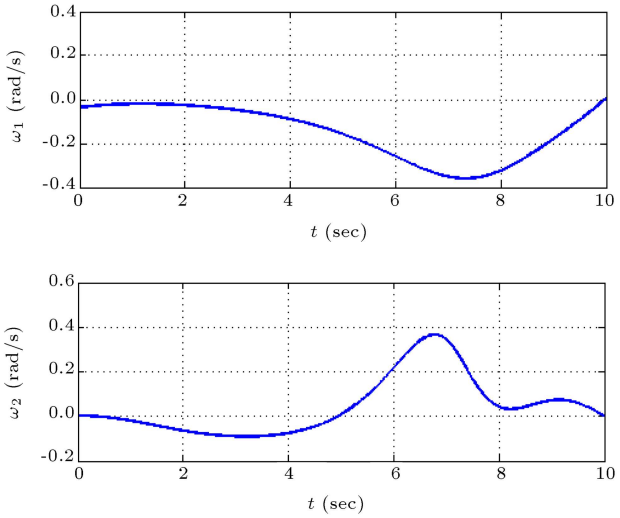

Figure 10. Angular velocity of joints 1 and 2.

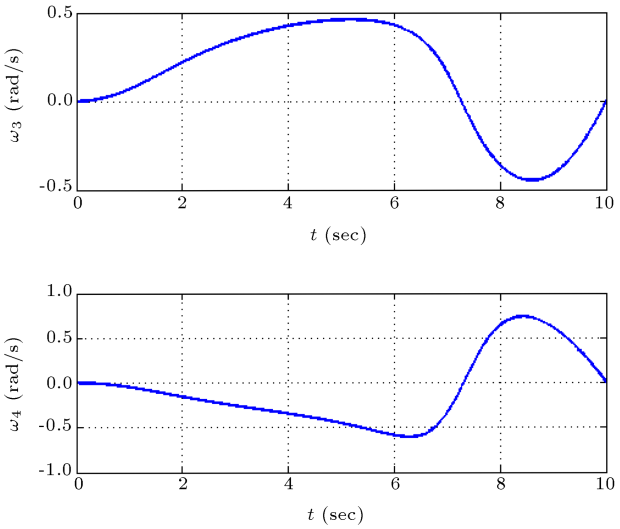

Figure 11. Angular velocity of joints 3 and 4.

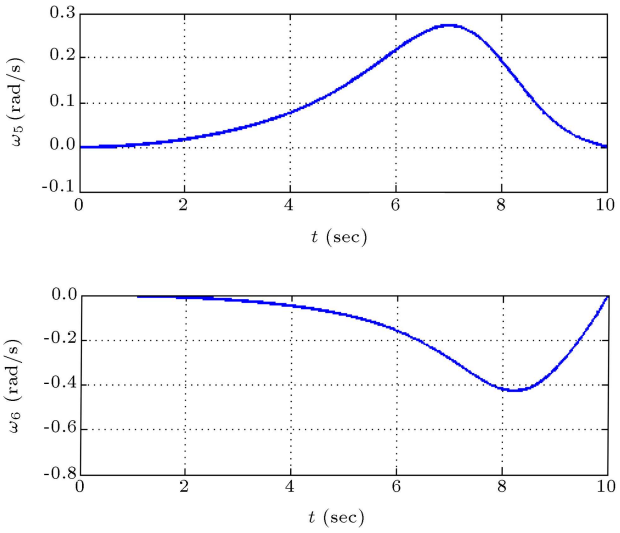

Figure 12. Angular velocity of joints 5 and 6.

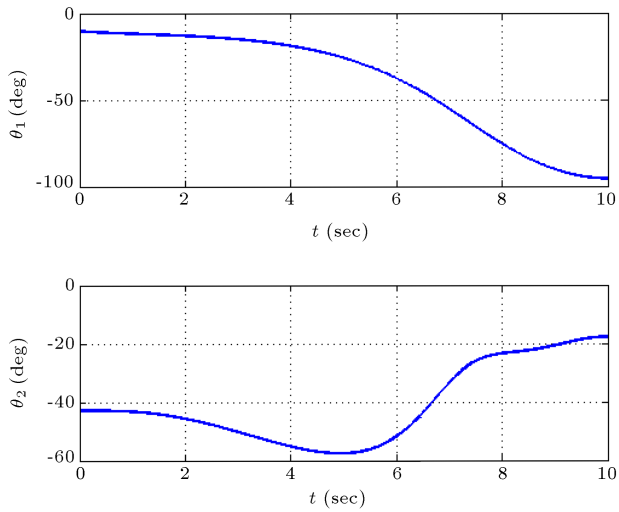

Figure 13. Angular position of joints 1 and 2.

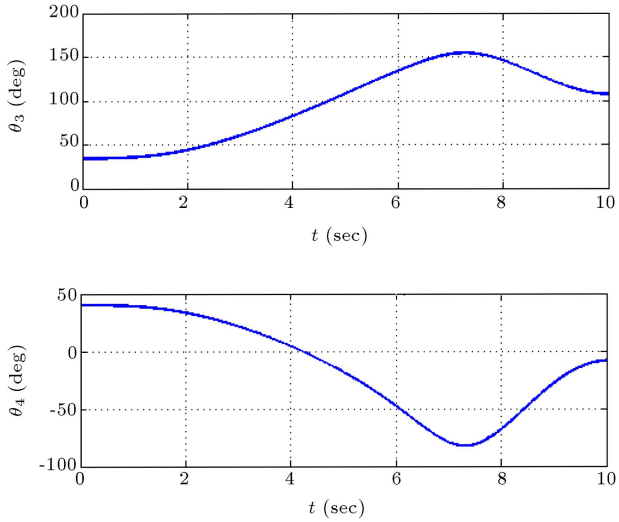

Figure 14. Angular position of joints 3 and 4.

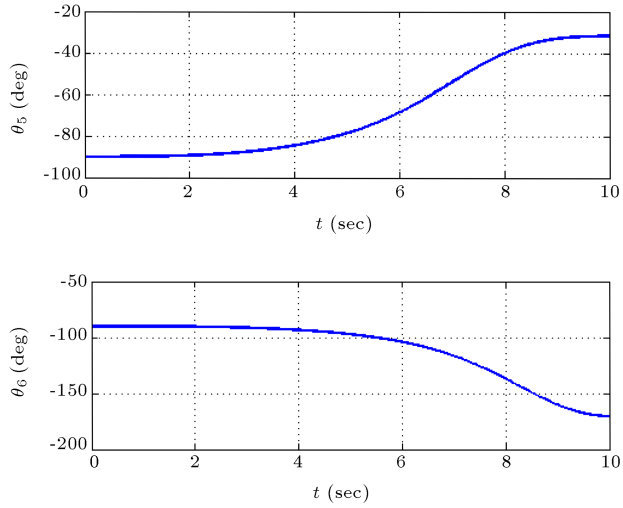

Figure 15. Angular position of joints 5 and 6.

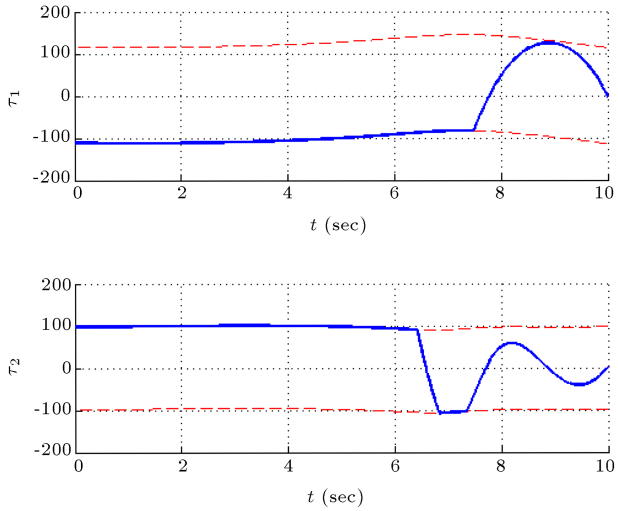

Figure 16. Torques of motors 1 and 2.

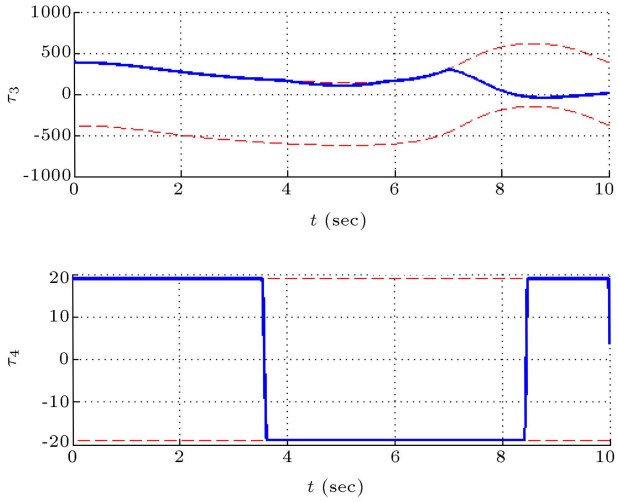

Figure 17. Torques of motors 3 and 4.

The values of torque of each motor are calculated through the SDRE algorithm and are plotted in Figures 16 to 18. The upper and lower values of torques are calculated by Equations 21 and 22 and are shown in these figures. These figures are plotted for maximum load carrying conditions. Moreover, the figures express that the motors work with a maximum value of torque at the beginning of motion.

Configuration links of the manipulator and the actual and desired linear path of the end-effector during the tracking motion are presented in Figure 19, and with a better view in Figure 20.

Tracking accuracy is selected to be $\delta = 0.022$ m, and according to both limitations on tracking error and motor torques, the dynamic load carrying capacity is obtained as DLCC = 1 kg. Figure 21 illustrates the tracking error as a function of time during the motion. Changes in characteristics of motors and allowable tracking error will affect the value of DLCC.

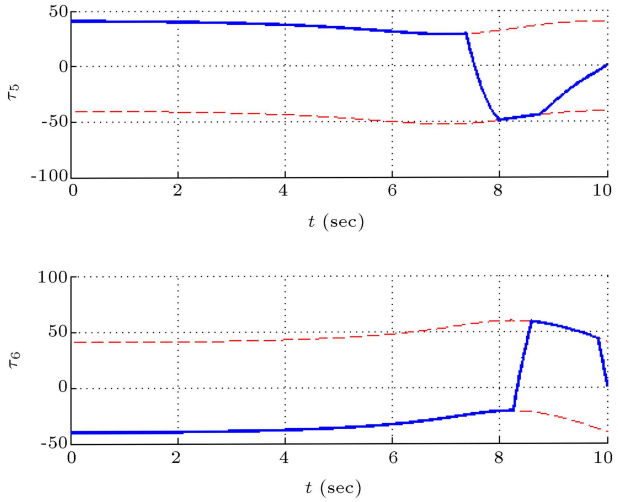

Figure 18. Torques of motors 5 and 6.

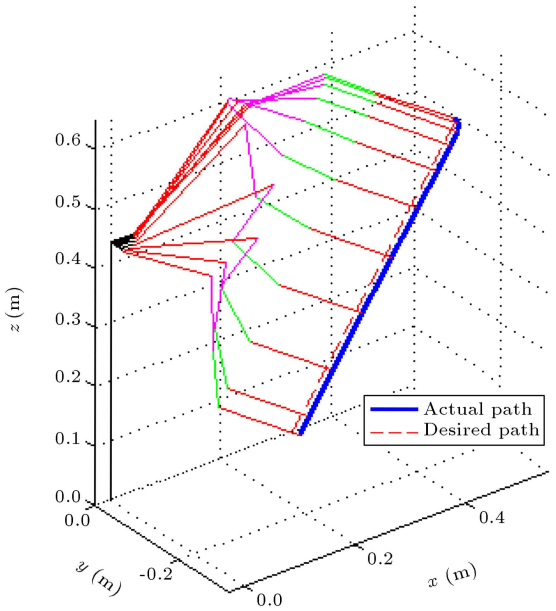

Figure 19. Configuration of robot during tracking.

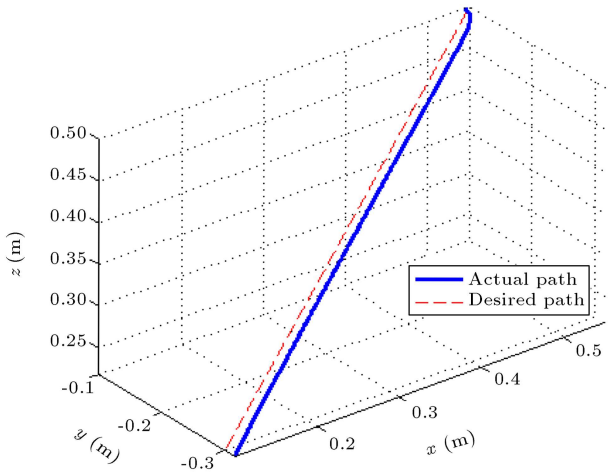

Figure 20. Desired and actual trajectory

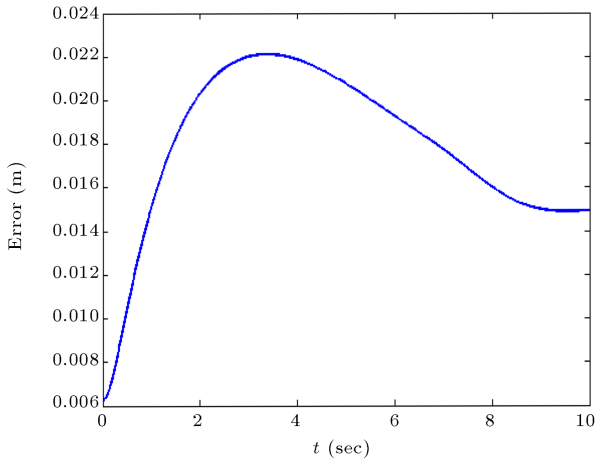

Figure 21. Tracking error.

CONCLUSION

In this paper, the state-dependent Riccati equation is discussed as a nonlinear optimal feedback controller. The power series approximation method has been employed for solving the SDRE problem. For a mobile robot, the dynamic load carrying capacity with consideration of tracking error and stability constraint has been obtained. Also, the DLCC of a 6R manipulator is calculated with tracking error consideration. Variations in R and Q matrixes change the value of the tracking error and control efforts. In order to reach better tracking accuracy, elements of matrix R must be decreased, but the period of simulation is increased and the motors come close to saturation conditions. It is seen that the tracking error is appeared as a function of both R and Q, and the tracking accuracy can be increased by changing these matrixes. Different state-dependent coefficient parameterization, which results in a different matrix, A, leads to an additional degree of freedom for the design controller and, as a result, different values of DLCC can be calculated. After appropriate state-dependent coefficient parameterization, the control design procedure using the SDRE method is systematic and done automatically. It is seen that the SDRE method is suitable for solving nonlinear closed loop optimal control problems and the DLCC can be determined using this method for both mobile and fixed robotic systems.

NOMENCLATURE

$A(x)$	state-dependent coefficient matrix
A_0	constant part of $A(x)$
$\Delta A(x)$	nonlinear part of $A(x)$
$g(x)$	nonlinear functions in $\Delta A(x)$

f, B	nonlinear functions in dynamic equations
$J(x)$	performance index
Q, R	states and control weighting matrixes
$X(x)$	the solution of SDRE
F	base and arm connecting point
L_0	the distance from F to the intersection point of the axis of symmetry with the driving wheel axis
θ_0	the heading angle of platform measured from X-axis of the world coordinates
θ_i	the angular displacements of links
τ_i	the torques exerted to joints
E	tracking error
δ	tracking accuracy
J	Jacobian matrix
J_{ij}	elements in dynamic equations
j_{ij}	elements of Jacobian matrix
x	vector of state variables
x_0	initial values of state variables
x_{zmp}, y_{zmp}	the coordination of zero moment point
x_d, y_d, z_d	desired position of end effector
x_f, y_f	the coordination of F
x_e, y_e, z_e	the coordination of E
q	the vector of generalized coordinates of the system
q_b	the vector of mobile base coordinates
q_m	the vector of manipulator coordinates
T	transformation matrix
n_x, n_y, n_z	
o_x, o_y, o_z	elements of transformation matrix
a_x, a_y, a_z	
p_x, p_y, p_z	
V	velocity vector of end effector
C	vector of centrifugal and Coriolis forces
$\bar{c}_i$	elements of C
D	inertia matrix of manipulator
d_{ij}	elements of inertia matrix
G	gravity force vector
g_i	elements of G
U	input control vector
u_i	input control torque of links (elements of U)
$U_{\max}, U_{\min}$	maximum and minimum of motor torques
U_s	stall torque of motors
ω_s	no load speed of motor

REFERENCES

1. Korayem, H. and Pilechian, A. "Maximum allowable load of elastic joint robots: Sliding mode control approach", *Amirkabir Journal of Science & Technol.*, **17**(65), pp. 75-82 (2007).
2. Korayem, M.H., Davarpanah, F. and Ghariblu, H. "Load carrying capacity of flexible joint manipulator with feedback linearization", *Int. J. Adv. Manuf. Technol.*, **29**(3-4), pp. 389-397 (2006).
3. Korayem, M.H. and Irani, M. "Maximum dynamic load determination of mobile manipulators via nonlinear optimal feedback", *Scientia Iranica, Trans. B, Mech. Eng.*, **17**(2), pp. 121-135 (2010).
4. Korayem, M.H., Najafi, Kh. and Bamdad, M. "Synthesis of cable driven robots dynamic motion with maximum load carrying capacities: iterative linear programming approach", *Scientia Iranica, Trans. B, Mech. Eng.*, **17**(3) pp. 229-239 (2010).
5. Korayem, M.H., Firouzy, S. and Heidari, A. "Dynamic load carrying capacity of mobile-base flexible-link manipulators feedback linearization control approach", *Proceedings of IEEE Int. Conference on Robotics and Biomimetics*, pp. 2172-2177 (2007).
6. Korayem, M.H., Heidari, A. and Nikoobin, A. "Maximum allowable dynamic load of flexible mobile manipulators using finite element approach", *Int. J. of Adv. Manuf. Technol.*, **36**, pp. 606-617 (2008).
7. Korayem, M.H., Azimirad, V., Nikoobin, A. and Boroujeni, Z. "Maximum load-carrying capacity of autonomous mobile manipulator in an environment with obstacle considering tip over stability", *Int. J. Adv. Manufacturing Technol.*, **46**(5-8), pp. 811-829 (2010).
8. Pearson, J.D. "Approximation methods in optimal control", *Journal of Electronics and Control*, **13**(5), pp. 453-465 (1962).
9. Wernli, A. and Cook, G. "Suboptimal control for the nonlinear quadratic regulator problem", *Automatica*, **11**, pp. 75-84 (1975).
10. Cloutier, J.R. and Cockburn, J.C. "The state-dependent nonlinear regulator with state constraints", *American Control Conference*, pp. 390-395 (2001).
11. Erdem, E.B. and Alleyne, A.G. "Experimental real-time SDRE control of an under actuated robot", *The 40th IEEE Conference on Design and Control*, Florida, pp. 2986-2991 (2001).
12. Innocenti, M., Baralli, F. and Salotti, F. "Manipulator path control using SDRE", *Proceedings of the American Control Conference*, pp. 3348-3352 (2000).
13. Xin, M., Balakrishnan, S.N. and Huang, Z. "Robust state dependent Riccati equation based robot manipulator control", *Proceedings of IEEE International Conference on Control Applications*, pp. 369-374 (2001).
14. Shawky, A., Ordys, A. and Gremble, M.J. "End-point control of a flexible-link manipulator using H-inf nonlinear control via state-dependent Riccati equation", *Proceedings of IEEE International Conference on Control Applications*, pp. 501-506 (2002).

15. Singh, N.M., Dubey, J. and Laddha, G. "Control of pendulum on a cart with state dependent Riccati equations", *Proceedings of World Academy of Science, Engineering and Technology*, **3**, pp. 676-676 (2008).

16. Cimen, T., *State-Dependent Riccati Equation (SDRE) Control: A Survey*, The International Federation of Automatic Control, pp. 3761-3775 (2008).

17. Beikzadeh, H. and Taghirad, H.D. "Nonlinear senseless speed control of PM synchronous motor via an SDRE observer-controller combination", *Proc. of the 4th IEEE Conference on Industrial Electronics and Applications*, Xian, China, pp. 3570-3575 (2009).

18. Beeler, S.C., *State-Dependent Riccati Equation Regulation of Systems with State and Control Nonlinearities*, NASA Langley Research Center, National Institute of Aerospace (2004).

19. Banks, H.T., Lewis, B.M. and Tran, H.T. "Nonlinear feedback controllers and compensators: a state-dependent Riccati equation approach", *Computational Optimization and Applications*, **37**(2), pp. 177-218 (2007).

20. Kim, J. and Chung, W.K. "Real time ZMP compensation method using null motion for mobile manipulator", *Proceedings of the IEEE International Conference on Robotics and Automation*, pp. 1967-1972 (2002).

21. Korayem, M.H. and Heidari, F.S. "Simulation and experiments for a vision-based control of a 6R robot", *Int. J. Adv. Manufacturing Technol.*, **41**(3-4), pp. 367-385 (2009).

BIOGRAPHIES

Moharam Habibnejad Korayem was born in Tehran Iran on April 21, 1961. He received his B.S. (Hon) and M.S. in Mechanical Engineering from the Amirkabir University of Technology in 1985 and 1987, respectively. He has obtained his Ph.D. degree in Mechanical Engineering from the University of Wollongong, Australia, in 1994. He is a Professor in Mechanical Engineering at the Iran University of Science and Technology. He has been involved with teaching and research activities in the robotics areas at the Iran University of Science and Technology for the last 15 years. His research interests includes dynamics of Elastic Mechanical Manipulators, Trajectory Optimization, Symbolic Modeling, Robotic Multimedia Software, Mobile Robots, Industrial Robotics Standard, Robot Vision, Soccer Robot, and the Analysis of Mechanical Manipulator with Maximum Load Carrying Capacity. He has published more than 300 papers in international journal and conference in the robotic area.

Mohsen Irani was born in Kashan, Iran on 22 July, 1980. He received his B.S. in Mechanical Engineering from the Isfahan University of Technology in 2002 and M.S. in Aerospace Engineering from the KNTU University of Technology in 2005. He is currently a Ph.D. student in Mechanical Engineering in the Iran University of Science and Technology, Tehran, Iran, since 2007. His research interests includes: Robotic Systems, Nonlinear Control, Optimal Control, Mobile Manipulators, Industrial Automation and Mechatronic Systems.

Saeed Rafee Nekoo was born in Tehran, Iran, on February, 12, 1984. He received the Associate of Mechanical Engineering from Jabbarian technical Junior College of Hamedan in 2004 and the B.S. in Mechanical Engineering from the Azad University of Tehran, South Branch in 2007. He is presently student of master of Mechanical Engineering in the Iran University of Science and Technology. His current research and interests include: Robotic, Control, Manufacturing, and Mechatronics systems.